

# Estimating long-term creep and shrinkage of high-strength concrete

M. Mazloom \*

*Civil Engineering Department, Shahid Rajaei University, Lavizan, P.O. Box 16785-163, Tehran 16788, Iran*

Received 14 March 2006; received in revised form 23 September 2007; accepted 24 September 2007

Available online 29 September 2007

## Abstract

This paper presents the development of formulas to estimate the long-term creep and shrinkage of high-strength concrete. The experimental part of the work focused on concrete mixes having a fixed water/binder ratio of 0.35 and a constant total binder content of 500 kg/m<sup>3</sup>. The percentages of silica fume that replaced cement in this research were: 0%, 6%, 8%, 10% and 15%. According to the experimental results some equations are proposed for predicting the time-dependent behaviour of high-strength concrete. Based upon a survey of published experimental data, the accuracy of the proposed equations compares favorably with that of several common methods, which were developed for estimating the creep and shrinkage of normal strength concrete. Also, according to the experimental work, it is shown that to improve the estimation of long-term deformations of high-strength concrete utilizing the ACI and CEB methods, the results of short-term tests should be substituted into them.

© 2007 Elsevier Ltd. All rights reserved.

**Keywords:** High-strength concrete; Silica fume; Creep; Shrinkage; Elastic modulus; Modeling

## 1. Introduction

The importance of creep and shrinkage is significant in that each, depending upon the concrete maturity at loading, can be two to four times larger than the elastic strain [1]. The problem of exact predicting the long-term deformations of high-strength concrete remains too. In fact, reliable estimation according to the existing models is not possible because they are developed for ordinary concrete and also the influence of aggregate cannot be estimated without tests. Therefore, it is desirable to develop means of estimating long-term deformations from short-term tests. In other words, if very accurate predictions of deformations are required, the long-term behaviour must be extrapolated, using an assumed time function, from creep and shrinkage tests performed on the prototype concrete. However, relatively simple prediction equations are required for design when the only factors known to the design engineer are specified concrete strength, age of load-

ing, probable ambient humidity and the volume to surface ratio of the member.

Clearly, the accuracy of the prediction of creep and shrinkage depends upon the form of the time function used. Neville et al. [2] have reviewed the various types of equations generally used, which are: power expression, logarithmic expression, exponential expression and hyperbolic expression. A combined power and hyperbolic form, suggested by Branson et al. [3], is also of interest. The present paper suggests improved prediction expressions derived from experimental results obtained by the author and verified against the test results of other investigators. It is worth noting that the final prediction expressions were published earlier [4]; however, they were not verified based upon a survey of the published experimental data. Also some recommendations are suggested for improving the exactness of the existing models for predicting the long-term creep and shrinkage of high-strength concrete.

## 2. Experimental details

The cementitious materials used were ordinary Portland cement (OPC) and silica fume (SF), their chemical compo-

\* Tel.: +98 21 77844025; fax: +98 21 22932423.

E-mail address: [MOOSPOON@yahoo.com](mailto:MOOSPOON@yahoo.com)

sitions and physical properties being given in Table 1. Details of the mix proportions for the concrete containing different levels of silica fume are given in Table 2. Crushed granite sand and gravel with a nominal maximum size of 10 mm were used as the aggregates. The control mix was cast using OPC, while the other mixes were prepared by replacing part of the cement with silica fume at four different replacement levels on mass-for-mass basis. The water/cement ratio and the slump of control high-strength concrete were 0.35 and  $100 \pm 10$  mm, respectively. The same water/binder ratio of 0.35 was used for the other concrete mixes with the same amount of slump. Consequently, the dosage of superplasticiser changed due to the effect of the different levels of silica fume. The superplasticiser used is based on melamine formaldehyde and lignosulfonate. For each mix, the following specimens were made: 24 100 mm cubes for compressive strength; eight  $80 \times 270$  (diameter  $\times$  length) mm cylinders for creep; four  $80 \times 270$  mm and four  $150 \times 300$  mm cylinders for shrinkage. The details of the experimental work including the actual mixes used, test procedures and the spread of the results were published earlier [4].

### 3. Modeling

The equation used by the author for predicting the creep of the investigated concrete mixes is a hyperbolic-power expression as follows:

Table 1  
Chemical composition and physical properties of cementitious materials

Item	Cementitious materials (%)	
	Ordinary Portland cement	Silica fume
SiO <sub>2</sub>	21.46	91.70
Al <sub>2</sub> O <sub>3</sub>	5.55	1
Fe <sub>2</sub> O <sub>3</sub>	3.46	0.9
CaO	63.95	1.68
MgO	1.86	1.8
Cl	–	0.08
SO <sub>3</sub>	1.42	0.87
K <sub>2</sub> O	0.54	–
Na <sub>2</sub> O	0.26	–
LOI	–	2
<i>Compounds</i>		
C <sub>3</sub> S	50.96	–
C <sub>2</sub> S	23.1	–
C <sub>3</sub> A	8.85	–
C <sub>4</sub> AF	10.53	–
<i>Fineness</i>		
SSA (m <sup>2</sup> /kg)	330	14,000

Table 2  
Mix proportions of concrete containing different levels of silica fume

Mix components	Concrete mixes				
	OPC	SF6	SF8	SF10	SF15
Cement (kg/m <sup>3</sup> )	500	470	460	450	425
Silica fume (kg/m <sup>3</sup> )	0	30	40	50	75
Superplasticiser (kg/m <sup>3</sup> )	8.17	9.78	10.62	11.71	13.34
Gravel: 1203 kg/m <sup>3</sup> , sand: 647 kg/m <sup>3</sup> , water: 175 kg/m <sup>3</sup> W/b = 0.35.					

$$C(t, t_0) = \frac{(t - t_0)^d}{A \cdot (t - t_0)^d + B} \quad (1)$$

or

$$Y = A \cdot X + B \quad (2)$$

where  $X = (t - t_0)^d$ ,  $Y = (t - t_0)^d / C(t, t_0)$ ,  $(t - t_0)$  is duration of loading and  $t_0$  is loading age. The same equation is utilized for predicting the shrinkage of the concrete mixes. According to the experimental data, the values  $X$  and  $Y$  can be measured at each time. A plot of  $Y$  against  $X$  gives a straight line of slope  $A$ , and the intercept on the ordinate is equal to  $B$ . In this stage, Eq. (2) can be drawn after assuming a specific value for  $d$ . In fact,  $d$  is a constant power and if  $d = 1$ , Eq. (1) becomes a simple hyperbolic expression. The experimental results published earlier [4] show that the suggestions of ACI committee 209-92 [5] for  $d$  are applicable for the creep and shrinkage of high-strength concrete. These values are 0.6 and 1, respectively. According to Eq. (1) when  $(t - t_0) \rightarrow \infty$ , the limiting specific creep  $C_u \rightarrow 1/A$  and thus the limiting creep can be obtained directly from experimental results. Therefore:

$$C(t, t_0) = \frac{(t - t_0)^{0.6}}{(t - t_0)^{0.6} + B \cdot C_u} \cdot C_u \quad (3)$$

It can be seen when  $B \cdot C_u \rightarrow (t - t_0)^{0.6}$ , one-half of the ultimate creep is expected to occur. This means, considering the time-dependent behaviour of concrete, both  $A$  and  $B$  are meaningful and each of them shows a specific characteristic of concrete. All these parameters for the specimens loaded at the age of 7 days are given in Table 3. According to this table, the relation between ultimate specific creep and the proportion of silica fume can be found utilizing regression analysis as follows:

$$C_u = -3.65SF + 103 \quad (R^2 = 0.9314) \quad (4)$$

where SF is the percentage of silica fume replaced cement. It is clear that as the proportion of silica fume increased, the ultimate creep decreased. This may happen because of improving the strength of concrete at the age of loading as a result of increasing the silica fume replacement level. In fact, some researchers believe that specimens having higher compressive strength show lower creep [6–8]. Also the relation between  $B \cdot C_u$  and the proportion of silica fume can be obtained in a similar manner as follows:

Table 3  
Creep parameters of the specimens loaded at the age of 7 days

Mix components	Concrete mixes				
	OPC	SF6	SF8	SF10	SF15
$B$	0.2387	0.2703	0.2868	0.2573	0.2096
$A$	0.0095	0.0117	0.0153	0.0155	0.0190
$R^2$	0.9795	0.9893	0.9846	0.9815	0.9954
$C_u = 1/A$	105.26	85.47	65.36	64.52	52.63
$B \cdot C_u$	25.11	23.1	18.75	16.60	11.03

$$B \cdot C_u = 26.5 - SF \quad (R^2 = 0.9304) \quad (5)$$

The age, or fraction developed concrete strength, at which the concrete is loaded is known to influence the magnitude of the creep strains. In this research, the ratio of the ultimate specific creep of the specimens loaded at the age of 28 days to the ones loaded at the age of 7 days ( $C_{u28}/C_{u7}$ ) are between 0.75 and 0.78 with the average value and standard deviation of 0.76 and 0.012, respectively. Consequently, Eq. (3) should be multiplied by a correction coefficient, which is 1 and 0.76 for the loading ages of 7 and 28 days, respectively. For the other loading ages, which are more than 7 days, the coefficient above may be interpolated or extrapolated from these two benchmarks by the following equation:

$$Y = 1.08 - 0.0114t_0 \quad (6)$$

where  $t_0$  is loading age. By substituting (4) and (5) into (3) and considering (6) the specific creep (Creep/MPa) equation becomes:

$$C(t, t_0) = \frac{(t - t_0)^{0.6}}{(t - t_0)^{0.6} + (26.5 - SF)} \cdot (103 - 3.65SF) \cdot Y \cdot (1E - 6) \quad (7)$$

It is worth noting that creep is considered to have two components: basic creep obtained from sealed samples and drying creep, which is calculated by subtracting the basic creep and the shrinkage strain from the total deformation of loaded unsealed samples stored at the required relative humidity. The dimensions of the specimen and also the relative humidity are not considered in Eq. (7) because the drying creeps of the high-strength specimens investigated here were negligible [4]. It is clear that the creep strain of a specimen subjected to a sustained compressive stress of  $\sigma$  (MPa) is equal to  $\sigma \cdot C(t, t_0)$ . Some researchers use creep coefficient [9], which is the ratio of creep at any age  $t$  after application of load at time  $t_0$  to the elastic strain at the age of applying the load  $t_0$ , so that:

$$\phi(t, t_0) = C(t, t_0) \cdot E_c(t_0) \quad (8)$$

where  $\phi$  is creep coefficient and  $E_c$  is the modulus of elasticity. The results of modulus of elasticity of concrete specimens containing different levels of silica fume, which were obtained in the creep tests, are shown in Table 4. In fact, the cylindrical specimens of  $80 \times 270$  mm height were loaded at the ages of 7 and 28 days. Because the modulus of elasticity is related to the level of applied stress and also loading rate, all the specimens of this research were subjected to a stress of 10 MPa and the time taken to apply it was about 10 min. It is worth noting that severe internal micro cracking takes place in a concrete compression specimen at a stress/strength ratio of 0.4–0.6, and below this limit there is a linear relation between creep and the applied stress [2]. In this research, the limitation above is considered and the stress/strength ratio was between 0.14 and 0.22. It is not surprising that, if cracking under high stress/strength ratios occurs, the creep behaviour changes.

Table 4  
7- and 28-day compressive strength and modulus of elasticity

Kind and age of concrete	Compressive strength (MPa)	Measured modulus (GPa)	Predicted modulus by Eq. (9) (GPa)
<i>OPC</i>			
7 days	46	28.8	30.2
28 days	58	34.4	34
<i>SF6</i>			
7 days	50.5	31	31.7
28 days	65	35.5	36
<i>SF8</i>			
7 days	52	31.2	32.2
28 days	68	37.3	36.8
<i>SF10</i>			
7 days	52	31.1	32.2
28 days	67.5	37	36.6
<i>SF15</i>			
7 days	53	31.5	32.5
28 days	70	38.1	37.3

As shown in Table 4, increasing the silica fume replacement level increases the modulus of elasticity of concrete. Although ACI 318-95 [10] prediction equation for the modulus of elasticity was developed from tests on a very different type of concrete, it has predicted the modulus of elasticity of the investigated specimens properly. This result is in agreement with the findings of Brooks [11]. It should be mentioned that sealed and drying specimens had similar values of elastic modulus. ACI 318-95 [10] presents the following equation to calculate the modulus of elasticity:

$$E_c = 4.7(f_c)^{0.5} \quad (9)$$

where  $f_c$  is the compressive strength of standard cylinder specimen of  $150 \times 300$  mm height in MPa and  $E_c$  is the modulus of elasticity in GPa. Because 100 mm cube specimens were utilized to measure the compressive strength, a factor of 0.9 has been used to estimate the equivalent cylinder strength. This factor is greater than the usual factor of 0.8 that is generally used for lower strength concrete, and it was chosen after considering the data presented by Imam et al. [12]. As explained earlier, the assumed shrinkage equation is quite similar to the one used for creep. It means:

$$\varepsilon_{sh}(t, t_0) = \frac{(t - t_0)}{A \cdot (t - t_0) + B} \quad (10)$$

or

$$\varepsilon_{sh}(t, t_0) = \frac{(t - t_0)}{(t - t_0) + B \cdot \varepsilon_{shu}} \cdot \varepsilon_{shu} \quad (11)$$

It should be mentioned that silica fume replacement level did not have any significant influence on ultimate shrinkage. This is in agreement with the finding of the others [13]. Its average value was 516 microstrain with the standard deviation of 14.24. All the shrinkage parameters for the  $80 \times 270$  mm specimens are given in Table 5. According

Table 5  
Shrinkage parameters of 80 × 270 mm high drying specimens

Mix components	Concrete mixes				
	OPC	SF6	SF8	SF10	SF15
<i>B</i>	0.0241	0.0268	0.0288	0.0325	0.0334
<i>A</i>	0.0019	0.0019	0.0020	0.0019	0.0020
<i>R</i> <sup>2</sup>	0.9983	0.9986	0.9978	0.9981	0.9982
$\varepsilon_{shu} = 1/A$	526	526	500	526	500
<i>B</i> · $\varepsilon_{shu}$	12.68	14.1	14.4	17.1	16.7

to this table, the relation between  $B \cdot \varepsilon_{shu}$  and the percentage of silica fume can be estimated using regression analysis as follows:

$$B \cdot \varepsilon_{shu} = 0.3SF + 12.6 \quad (R^2 = 0.79) \quad (12)$$

Therefore, the shrinkage equation is

$$\varepsilon_{sh}(t, t_0) = \frac{(t - t_0)}{(t - t_0) + (0.3SF + 12.6)} \cdot (516E - 6) \quad (13)$$

Because of the very low moisture movement from the surface of very large and carbonated members, their long-term creep and shrinkage always decrease. To investigate the minimum long-term deformation of these members, the creep and shrinkage of some sealed specimens, which are called basic creep and autogenous shrinkage respectively, are studied in this research. It should be emphasized that autogenous shrinkage is definitely present and not negligible for high-strength concrete [14]. The shrinkage parameters of the sealed specimens and also the sealed/drying shrinkage ratios of 80 × 270 mm high specimens are given in Tables 6 and 7, respectively. According to Table 7, the effect of silica fume on ultimate sealed/drying shrinkage ratio can be calculated using regression analysis as follows:

$$Y = 0.014SF + 0.39 \quad (\text{for sealed specimens}) \quad (14)$$

In this research, the average ratio of the ultimate shrinkage of the 150 × 300 mm high specimens to 80 × 270 mm high specimens ( $\varepsilon_{shu2}/\varepsilon_{shu1}$ ) is 0.88. Consequently, Eq. (13) should be multiplied by a correction coefficient, which is

Table 6  
Shrinkage parameters of sealed specimens

Mix components	Concrete mixes				
	OPC	SF6	SF8	SF10	SF15
<i>B</i>	0.1849	0.1298	0.1325	0.1503	0.1350
<i>A</i>	0.0049	0.0042	0.0039	0.0036	0.0032
<i>R</i> <sup>2</sup>	0.9961	0.9972	0.9964	0.9986	0.9960
$\varepsilon_{shu} = 1/A$	204	238	256	278	313

Table 7  
Ultimate sealed/drying shrinkage ratio of 80 × 270 mm high specimens

Mix components	Concrete mixes				
	OPC	SF6	SF8	SF10	SF15
$\varepsilon_{shu1}/\varepsilon_{shu2}$	0.40	0.46	0.50	0.54	0.61

1 and 0.88 for 80 × 270 mm high specimens (volume/surface ratio = 20 mm) and 150 × 300 mm high specimens (volume/surface ratio = 37.5 mm), respectively. For the other specimen sizes, the coefficient above may be interpolated or extrapolated from these two benchmarks by the following equation:

$$Y = 1.14 - 0.007(V/S) \geq 0.014SF + 0.39 \quad (\text{for drying specimens}) \quad (15)$$

where  $V/S$  is the volume/surface ratio of the specimen in mm. It is evident that the  $Y$  coefficient in very large members can not be lower than the one in sealed specimens. This fact is considered in Eq. (15). As a result, the ultimate shape of the shrinkage model is

$$\varepsilon_{sh}(t, t_0) = \frac{(t - t_0)}{(t - t_0) + (0.3SF + 12.6)} \cdot Y \cdot (516E - 6) \quad (16)$$

#### 4. Verification of the proposed models

Because Eqs. (7) and (16) have been developed from the limited data set obtained by the author, they are verified based upon a survey of published experimental data in this section. Also these equations are compared with that of several common methods, which were developed for estimating the creep and shrinkage of normal strength concrete.

##### 4.1. Creep model

In this part of the work the experimental results of creep in specimens loaded at the ages of 7 and 28 days are used to check Eq. (7). Also the results are compared with the ACI [5], CEB [15], Bazant and Baweja [16] and Gardner and Zhao [1] prediction methods, which were developed for the creep of ordinary concrete. These prediction models are

$$C(t, t_0) = 1/E(t_0) \cdot t^{0.6}/(10 + t^{0.6}) \cdot \phi(u) \quad (\text{ACI209-92}) \quad (17)$$

where  $\phi(t)$  is ultimate creep coefficient; and

$$C(t, t_0) = 1/E(t = 28) \cdot [t/(\beta_h + t)]^{0.3} \cdot \phi(u) \quad (\text{CEB-FIP}) \quad (18)$$

where  $\beta_h$  is the shape function of the specimen; and

$$J(t, t') = q_1 + C_0(t, t') + C_d(t, t', t_0) \quad (\text{Bazant and Baweja}) \quad (19)$$

where  $J(t, t')$  is compliance function,  $q_1$  is instantaneous deformation,  $C_0(t, t')$  is basic creep and  $C_d(t, t', t_0)$  is drying creep; and

$$C(t, t_0) = 1/E(t_0) \cdot \{[7.27 + \ln(t)]/17.18\} \cdot [1.57 + 2.98 \cdot (f_{cm28}/f_{cm10}) \cdot (25/f_{cm28})^{0.5}] \cdot (1 - h^2) \cdot \{t/[t + 0.1 \cdot (V/S)^2]\} \quad (20)$$

(Gardner and Zhao)

where  $f_{cm10}$  is concrete strength at the age of loading and  $h$  is relative humidity as a decimal.

It is worth emphasizing that in Bazant and Baweja method [16] the compliance function, which is elastic strain plus creep per unit of stress, should be utilized. As shown in Fig. 1, Eq. (7) and the ACI, CEB, Bazant and Baweja, and Gardner and Zhao methods are compared for predicting the creep of high-strength concrete containing different levels of silica fume. In fact, the referenced models of ACI,

CEB, Bazant and Baweja, and Gardner and Zhao have been developed for a wider range of concrete mixes and it is understandable that they exhibit more scatter for a smaller dataset of higher strength concrete considered. To compare these models numerically, the error coefficient method is used. According to Neville et al. [2] the error coefficient  $M$  for creep at any age  $t$ , for concrete subjected to load at an earlier age  $t_0$ , is defined as:

$$M = \frac{1}{C_{avr}(t, t_0)} \cdot \sum \left[ \frac{[C_o(t, t_0) - C_p(t, t_0)]^2}{n} \right]^{0.5} \quad (21)$$

where  $C_o(t, t_0)$  is observed creep,  $C_p(t, t_0)$  is predicted creep and  $C_{avr}(t, t_0)$  is mean observed creep for a number of observations  $n$ . It should be emphasized that, according

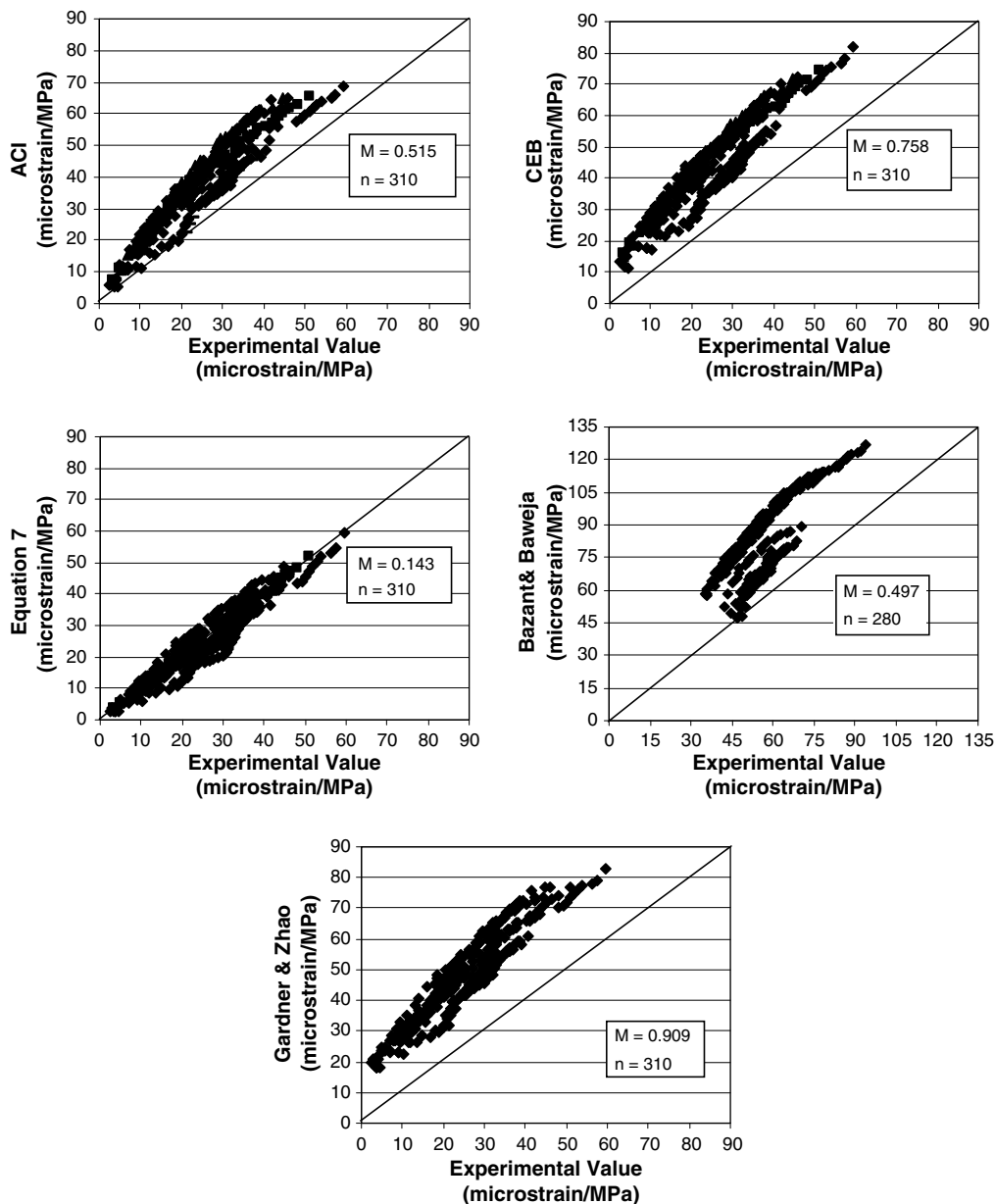


Fig. 1. Comparing different creep models according to the experimental work.



to Neville et al. [2], variable  $n$  in Eq. (21) is inside the square root. In fact, the accuracy of different prediction methods can be assessed in terms of error coefficient and a value of 0.15 can be assumed acceptable [2].

Fig. 1 shows that the error coefficients of Eq. (7), ACI [5], CEB [15], Bazant and Baweja [16], and Gardner and Zhao [1] for the specimens investigated here were 0.143, 0.515, 0.758, 0.497, and 0.909, respectively. It is clear that just the error coefficient of Eq. (7) is lower than 0.15. Also the experimental results existing in the literature are used to compare the exactness of the five methods above in predicting the creep of high-strength concrete. The comparison of

Eq. (7), ACI [5], CEB [15], Bazant and Baweja [16], and Gardner and Zhao [1] with the experimental results of Larrard and Roy [17]; Dilger and Wang [18]; Brooks and Wainwright [19]; Bilodeau et al. [20]; Buil and Acker [21]; Collins [22]; Ngab, Nilson and Slate [23]; Schrage and Springenschmid [24]; Brooks and Al-Qarra [25]; Giaccio et al. [26]; Parrot [27]; Burg and Ost [28]; Marzouk [29] is shown in Fig. 2. It is worth noting that although these tests were carried out on different mixes and different specimen sizes, all the prediction models investigated here have considered the dimensions of the specimens and the concrete specifications. As shown in Fig. 2, the error coefficients

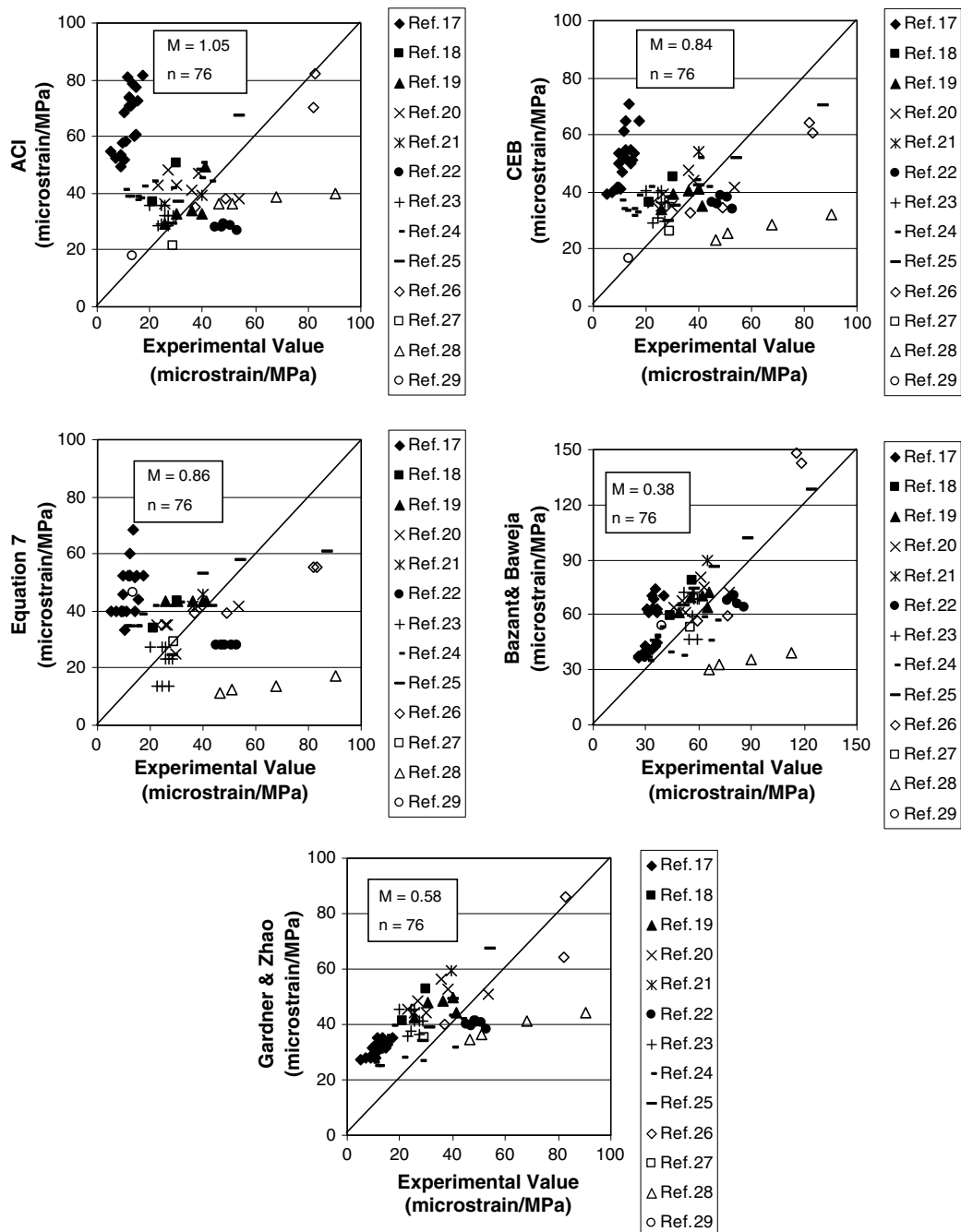


Fig. 2. Comparing different creep models according to the published data.

of all the five methods are more than 0.15. It means that generally reliable estimation according to these models is not possible because the influence of aggregate cannot be estimated without tests. Therefore, it may be desirable to develop means of estimating long-term creep from short-term tests.

#### 4.2. Shrinkage model

In this part of the investigation the experimental results of shrinkage in cylindrical specimens of  $80 \times 270$  mm and  $150 \times 300$  mm height are used to check Eq. (16). Also the results are compared with the ACI [5], CEB [15], Bazant and Baweja [16], and Gardner and Zhao [1] prediction methods, which were developed for the shrinkage of ordinary concrete. These prediction equations are:

$$\varepsilon_{sh}(t) = t/(35 + t) \cdot \varepsilon_{sh}(u) \quad (\text{ACI 209-92}) \quad (22)$$

where  $\varepsilon_{sh}(u)$  is ultimate shrinkage; and

$$\varepsilon_{sh}(t) = [t/(\beta_{sh} + t)]^{0.5} \cdot \varepsilon_{sh}(u) \quad (\text{CEB-FIP}) \quad (23)$$

where  $\beta_{sh}$  is the shape function of the specimen; and

$$\varepsilon_{sh}(t) = \varepsilon_{sh}(u) \cdot k_h \cdot s(t) \quad (\text{Bazant and Baweja}) \quad (24)$$

where  $k_h$  and  $s(t)$  are relative humidity function and time function, respectively; and

$$\varepsilon_{sh}(t) = \varepsilon_{sh}(u) \cdot \beta(h) \cdot \beta(t) \quad (\text{Gardner and Zhao}) \quad (25)$$

where  $\beta(h)$  and  $\beta(t)$  are relative humidity function and time function, respectively.

As shown in Fig. 3, Eq. (16) and the Gardner and Zhao model present the shrinkage of high-strength concrete containing different levels of silica fume properly. To compare these models numerically, similar to creep equations, the error coefficient  $M$  is used. Fig. 3 shows that the error coefficients of Eq. (16), ACI [5], CEB [15], Bazant and Baweja

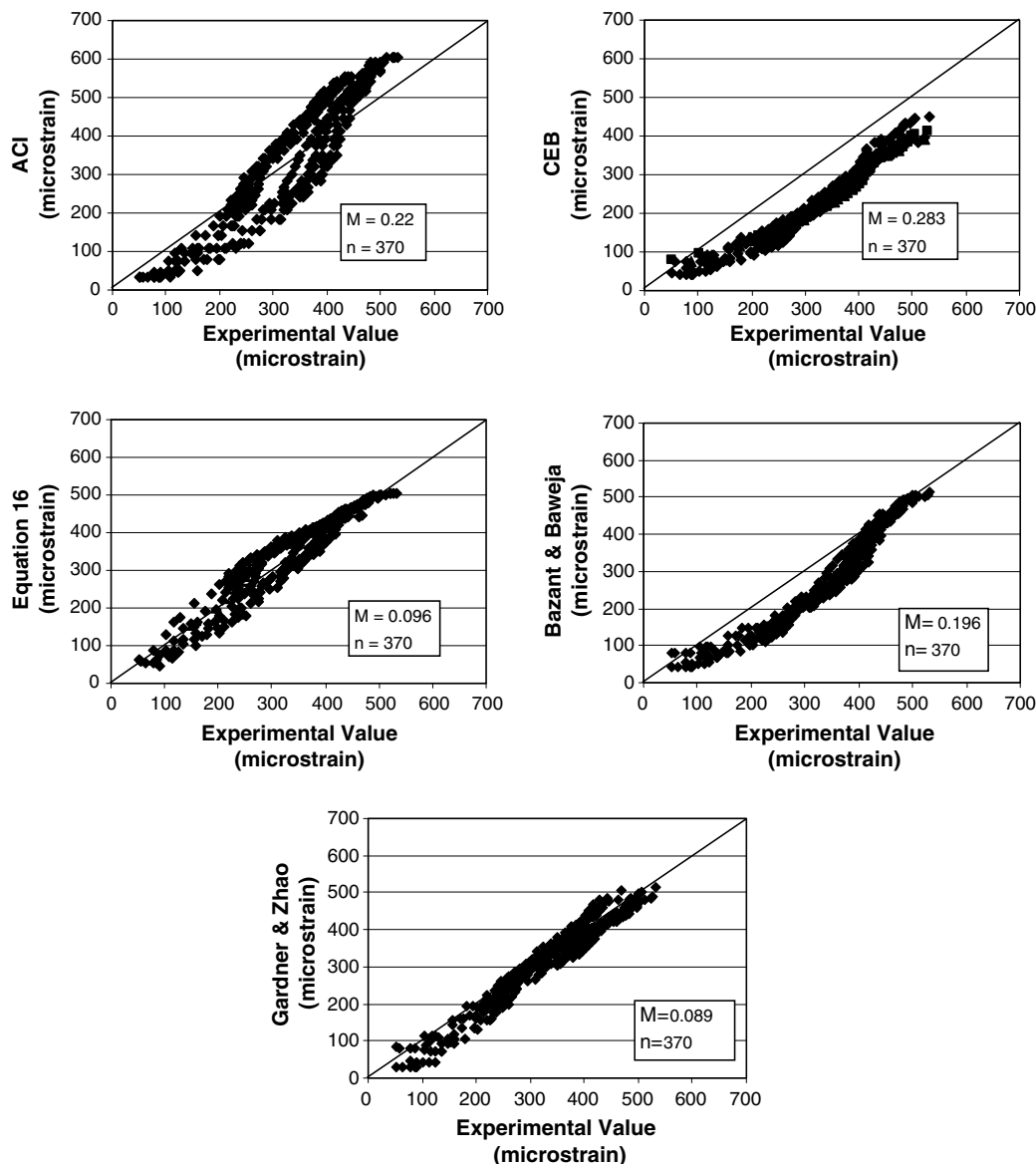


Fig. 3. Comparing different shrinkage models according to the experimental work.

[16], and Gardner and Zhao [1] for the specimens investigated here were 0.096, 0.22, 0.283, 0.196, and 0.089, respectively.

Also, the experimental results existing in the literature are used to compare the exactness of the five methods above in predicting the shrinkage of high-strength concrete. The comparison of Eq. (16), ACI [5], CEB [15], Bazant and Baweja [16], and Gardner and Zhao [1] with the experimental results of Larrard and Roy [17]; Dilger

and Wang [18]; Brooks and Wainwright [19]; Bilodeau et al. [20]; Buil and Acker [21]; Collins [22]; Ngab, Nilson and Slate [23]; Schrage and Springenschmid [24]; Brooks and Al-Qarra [25]; Giaccio, Giovambattista, Rocco and Zerbino [26]; Parrot [27]; Burg and Ost [28]; Larrard and Acker [30] is shown in Fig. 4. It is worth noting that although these tests were carried out on different mixes and different specimen sizes, all the prediction models investigated here have considered the dimensions of the

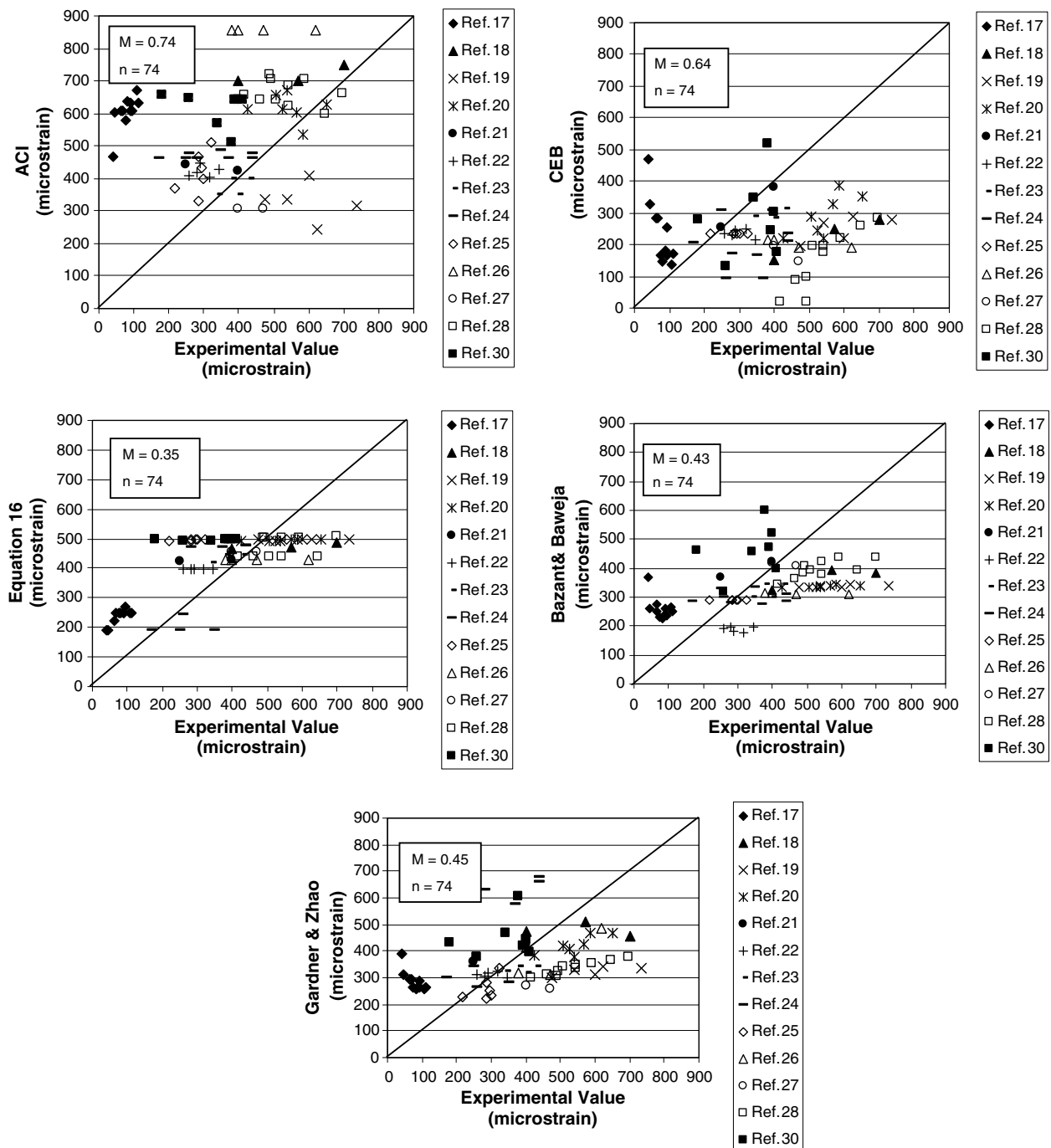


Fig. 4. Comparing different shrinkage models according to the published data.



specimens and the concrete specifications. As shown in Fig. 4, although the error coefficient of all the five methods are more than 0.15, the error coefficients of the ACI [5], CEB [15], Bazant and Baweja [16], and Gardner and Zhao [1] are 2.11, 1.83, 1.23, and 1.29 times more than the one presented by Eq. (16). In fact, the referenced methods of ACI, CEB, Bazant and Baweja, and Gardner and Zhao have been developed for a wider range of concrete mixes and it is understandable that they exhibit more scatter for the smaller data set of higher strength concrete considered.

## 5. Estimating long-term deformations from short-term tests

Close prediction of the future creep and shrinkage is impossible without short-term measurements on the given concrete [31]. To determine the shrinkage and creep characteristics of a prototype concrete, it is necessary to continue measurements for a duration sufficiently long to minimize perturbation effects due to using not matured results. According to Figs. 1–4 of the previous paper [4], the minimum time duration of 56 days is suggested for short-term tests of high-strength concrete mixes investigated here.

### 5.1. Creep

The ACI and CEB prediction methods for creep presented earlier, which are linear product models, can be shown by the following equation:

$$C(t) = F(t) \cdot C_u \quad (26)$$

where  $F(t)$  and  $C_u$  are time function and ultimate specific creep, respectively. The Bazant and Baweja [16], and Gardner and Zhao [1] models are more complicated and cannot be summarized and shown by this equation. Using Eq. (26) for  $t_1$  and  $t_2$ ,  $C_u$  can be eliminated to give:

$$C(t_2) = C(t_1) \cdot \frac{F(t_2)}{F(t_1)} \quad (27)$$

where  $t_1$  is the last time when creep is measured in the laboratory and  $t_2$  is the time after  $t_1$  that creep will be estimated. Consequently, after measuring the specific creep at time  $t_1$  in the laboratory, Eq. (27) can be used for estimating specific creep at any time  $t_2$  after  $t_1$ . To check this suggestion using the ACI and CEB models, the measured specific creep in the laboratory at the ages of  $t_2 = 165$ ,  $t_2 = 26$  and  $t_2 = 403$  days for the specimens loaded at the age of 7 days and also the measured specific creep at the ages of  $t_2 = 173$ ,  $t_2 = 275$  and  $t_2 = 404$  days for the specimens loaded at the age of 28 days are compared to their estimated values from Eq. (27) with the assumption of short-term test duration = 56 days. The results can be observed in Fig. 5. It is clear that the error coefficients of the ACI and CEB models have improved and they became about 0.17 in both methods. As a result, this suggestion

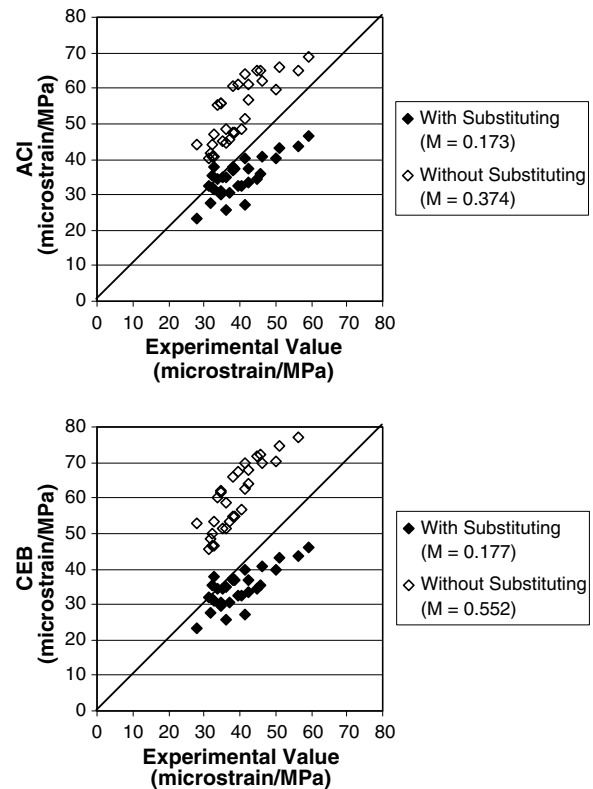


Fig. 5. Effect of substituting short-term tests into the existing creep models.

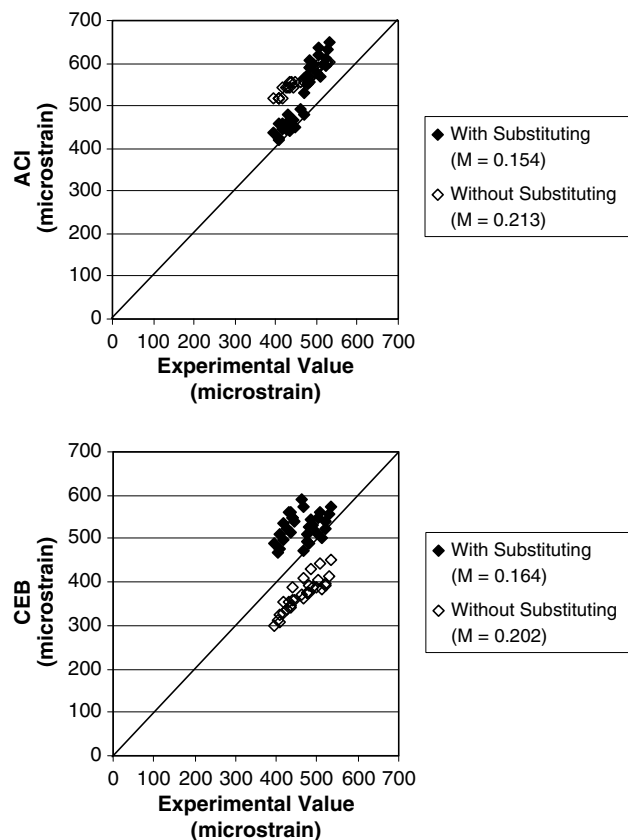


Fig. 6. Effect of substituting short-term tests into the existing shrinkage models.

can be used for more exact estimation of creep in high-strength concrete.

## 5.2. Shrinkage

The ACI and CEB prediction models presented earlier for shrinkage at time  $t_2$ , similar to the creep equations, can be shown by the following equation:

$$\varepsilon_{sh}(t_2) = \varepsilon_{sh}(t_1) \cdot \frac{F(t_2)}{F(t_1)} \quad (28)$$

Consequently, after measuring shrinkage at time  $t_1$  in the laboratory, Eq. (28) can be used for estimating shrinkage at any time  $t_2$  after  $t_1$ . To check this suggestion using the ACI and CEB models, the measured shrinkage in the laboratory at the ages of  $t_2 = 263$ ,  $t_2 = 423$  and  $t_2 = 594$  days are compared to their estimated values from Eq. (28) with the assumption of short-term test duration = 56 days. The results can be observed in Fig. 6. It is clear that the error coefficients of the ACI and CEB models have improved and they became about 0.16 in both methods. As a result, this suggestion can be used for more exact estimation of shrinkage in high-strength concrete.

## 6. Conclusions

According to the experimental work and published data, some equations have been developed for estimating the long-term creep and shrinkage of high-strength concrete. The accuracy of the proposed equations compares favorably with that of several common methods, which were developed for estimating the creep and shrinkage of normal strength concrete. Because of the very low moisture movement from the surface of very large and carbonated members, the proposed equations are calibrated by the results of the sealed laboratory-sized specimens to be used for these members.

If accurate estimate of long-term deformations is required, it is necessary that tests be performed on the prototype concrete and long-term strains be extrapolated from short-term tests. According to the experimental work on high-strength concrete, the minimum time duration of 56 days is suggested for short-term tests. Also, the proposed time functions of both the ACI and CEB can be used for this extrapolation. In fact, because this extrapolation is sensibly independent of mix proportions, type of aggregate, size of specimen and age at loading, it represents a suitable balance between simplicity and accuracy.

## References

- [1] Gardner NJ, Zhao JW. Creep and shrinkage revisited. *ACI Mater J* 1993;90(3):236–45.
- [2] Neville AM, Dilger WH, Brooks JJ. *Creep of plain and structural concrete*. London and New York: Springer; 1983.
- [3] Branson DE, Meyers BL, Kripanarayanan KM. Time dependent deformation of non-composite and composite sand-lightweight prestressed concrete structures. Iowa Highway Commission research report No. 69-1, Project No. HR-137, Phase I report, Iowa City, University of Iowa, 1969.
- [4] Mazloom M, Ramezaniapour AA, Brooks JJ. Effect of silica fume on mechanical properties of high-strength concrete. *Cement Concrete Comp* 2004;26:347–57.
- [5] ACI Committee 209. Prediction of creep, shrinkage and temperature effects in concrete structures, *ACI Manual of concrete practice*, Part 1, 1997, 209R 1-92.
- [6] Shah SP, Ahmad SH. *High performance concrete and applications*. London: Edward Arnold; 1994.
- [7] Neville AM. *Properties of concrete*. Edinburgh: Longman; 1995.
- [8] Khan AA, Cook WD, Mitchell D. Creep, shrinkage, and thermal strains in normal, medium, and high-strength concretes during hydration. *ACI Mater J* 1997;94(2):156–63.
- [9] Cusson D, Hooegeeve T. An experimental approach for the analysis of early-age behaviour of high-performance concrete structures under restrained shrinkage. *Cement Concrete Res* 2007;37: 200–9.
- [10] ACI Committee 318. Building code requirements for reinforced concrete, American Concrete Institute; 1995.
- [11] Brooks JJ. How admixtures affect shrinkage and creep. *Magazine of the American Concrete Institute-an international technical society*, April 1999, 35–8.
- [12] Imam M, Vandewalle L, Mortelmans F. Are current concrete strength tests suitable for high strength concrete? *Mater Struct* 1995;28:384–91.
- [13] Akkaya Y, Ouyang C, Shah SP. Effect of supplementary cementitious materials on shrinkage and crack development in concrete. *Cement Concrete Comp* 2007;29:117–23.
- [14] Lee Y, Yi ST, Kim MS, Kim JK. Evaluation of a basic creep model with respect to autogenous shrinkage. *Cement Concrete Res* 2006;36:1268–78.
- [15] CEB-FIP Model Code for concrete structures, Evaluation of the time dependent behavior of concrete, *Bulletin d'Information No. 199*, Comité Européen du Béton/Fédération Internationale de la Précontrainte, Lausanne, 1999.
- [16] Bazant ZP, Baweja S. Short form of creep and shrinkage prediction model B3 for structures of medium sensitivity. *Mater Struct* 1996;29:587–93.
- [17] De Larrard F, Le Roy R. The influence of mix-composition on the mechanical properties of silica fume high-performance concrete. In: *Proceedings, fourth international ACI-CANMET conference on fly ash, silica fume, slag and natural pozzolans in concrete*, Istanbul; 1992. p. 965–86.
- [18] Dilger WH, Wang C. Time dependent properties of high-performance concrete. In: *Proceedings of the 8th FIP congress*, Amsterdam, Netherlands; 1998. p. 59–63.
- [19] Brooks JJ, Wainwright PJ. Properties of ultra-high-strength concrete containing a superplasticizer. *Mag Concrete Res* 1983;35(125): 205–13.
- [20] Bilodeau A, Carrette GG, Malhotra VM. Mechanical properties of non-air entrained, high-strength concrete incorporating supplementary cementing materials. *Division Report MSL 89-129*, Mineral Sciences Laboratories, CANMET, Canada; 1989.
- [21] Buil M, Acker P. Creep of a silica fume concrete. *Cement Concrete Res* 1985;15:463–6.
- [22] Collins TM. Proportioning high-strength concrete to control creep and shrinkage. *ACI Mater J* 1989;86(6):576–80.
- [23] Ngab AS, Nilson AH, Slate FO. Shrinkage and creep of high-strength concrete. *ACI J* 1981;78(4):255–61.
- [24] Schrage I, Springenschmid R. Creep and shrinkage data of high-strength concrete. In: *Proceedings, 4th international symposium on high-strength/high-performance concrete*, Paris, France; 1996. p. 331–8.
- [25] Brooks JJ, Al-Qarra H. Assessment of creep and shrinkage of concrete for the Flintshire Bridge. *Struct Eng* 1999;77.
- [26] Giaccio G, Giovambattista A, Rocco C, Zerbino R. Compressive creep of high strength concrete. In: Bazant ZP, Carol I, editors. *Creep*

- and shrinkage of concrete, RILEM-Symposium. London: E and FN Boundary Row. p. 511–6.
- [27] Parrott LJ. The properties of high-strength concrete, Technical Report, Cement and Concrete Association, TRA 417, 1969.
- [28] Burg RG, Ost BW. Engineering properties of commercially available high-strength concretes. Research and Development Bulletin RD104T. Skokie (IL): Portland Cement Association; 1992.
- [29] Marzouk H. Creep of high-strength concrete and normal-strength concrete. *Mag Concrete Res* 1991;43(155):121–6.
- [30] De Larrard F, Acker P. Free deformations of high performance concrete. *Seminaire sur la Durabilite des BHP*, Cachan, 1990.
- [31] Bazant ZP. Prediction of concrete creep and shrinkage: past, present and future. *Nucl Eng Des* 2001;203:27–38.